Supplementary Figure 1

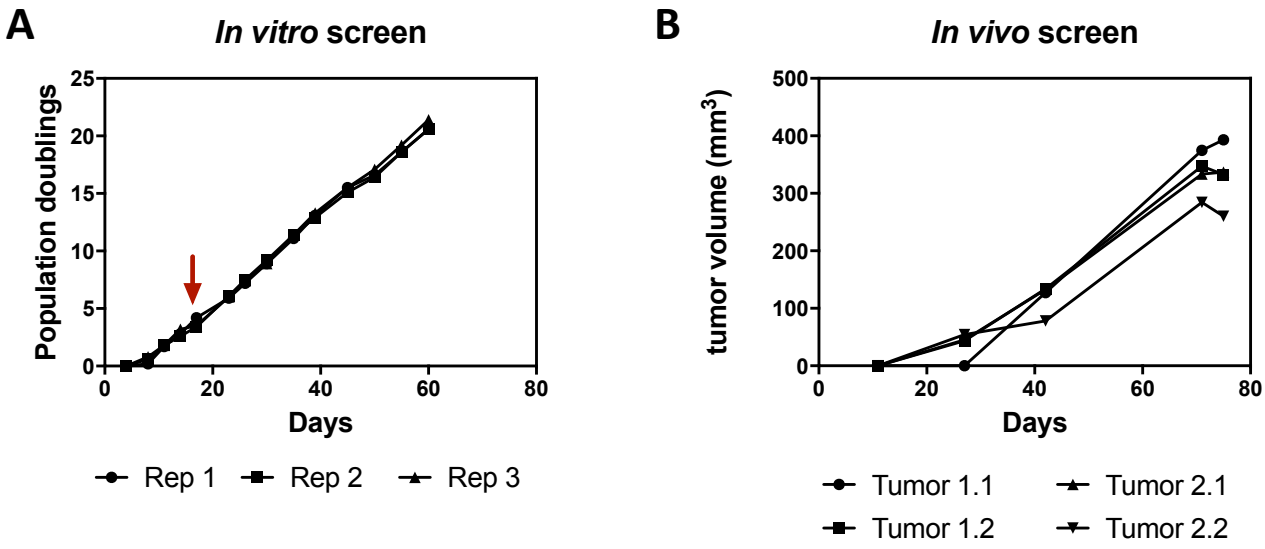

Figure S1. Growth curves during parallel *in vitro* and *in vivo* screening. (A) Three independent library transductions were performed, and after 4 population doublings (red arrow), cells were split parallel *in vitro* and *in vivo* screens. Cells were kept in continuous tissue culture for 20 population doublings (PDs). (B) For every biological replicate (independent viral transduction), two NOD-SCID mice were injected subcutaneously with 5 million cells each. Tumors were allowed to grow to at least 300 mm3 before harvest. Since the tumor 3.2 (*in vitro* replicate 3, tumor 2) exhibited significant delay in growth compared to the others, tumors from replicate 3 were not included in the final analysis.

Supplementary Figure 2

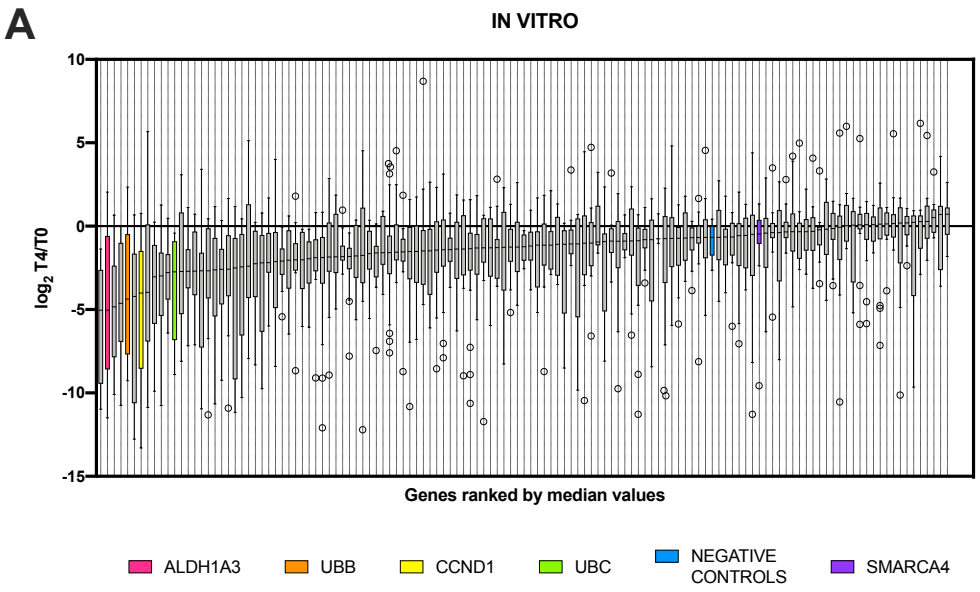

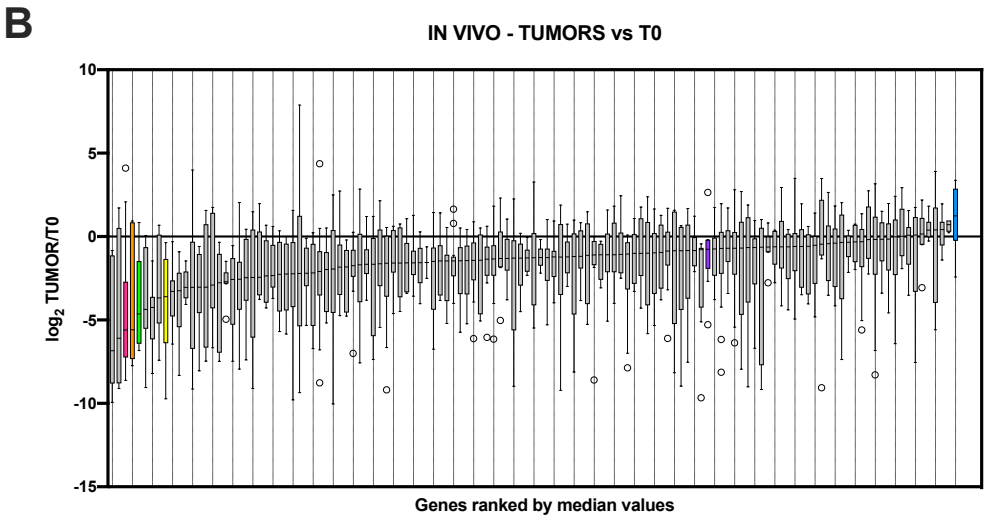

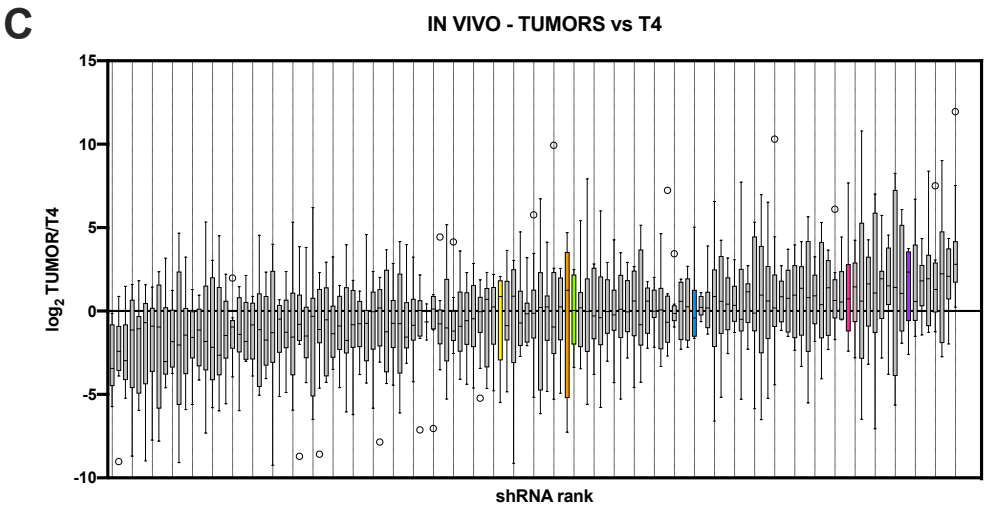

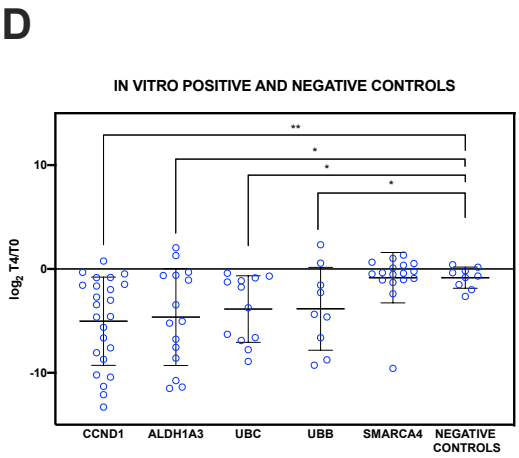

Figure S2. Behavior of control shRNAs in the parallel *in vitro* and *in vivo* pooled shRNA screen. Boxplots showing range of log2 T4/T0 values (A), log2 TUMOR/T0 values (B), and log2 TUMOR/T4 values (C) for all shRNAs for each gene. Outliers as defined by the Tukey method are indicated by points. Select genes which were either deliberately included as controls or are inherent biological controls are highlighted by indicated colors. (D) Comparison of log2 T4/T0 values of biological controls to negative controls (shNTC, non-mammalian shRNA, and shGFP as a group). P-values were calculated by unpaired t-tests.

Supplementary Figure 3A - Page 1 of 8

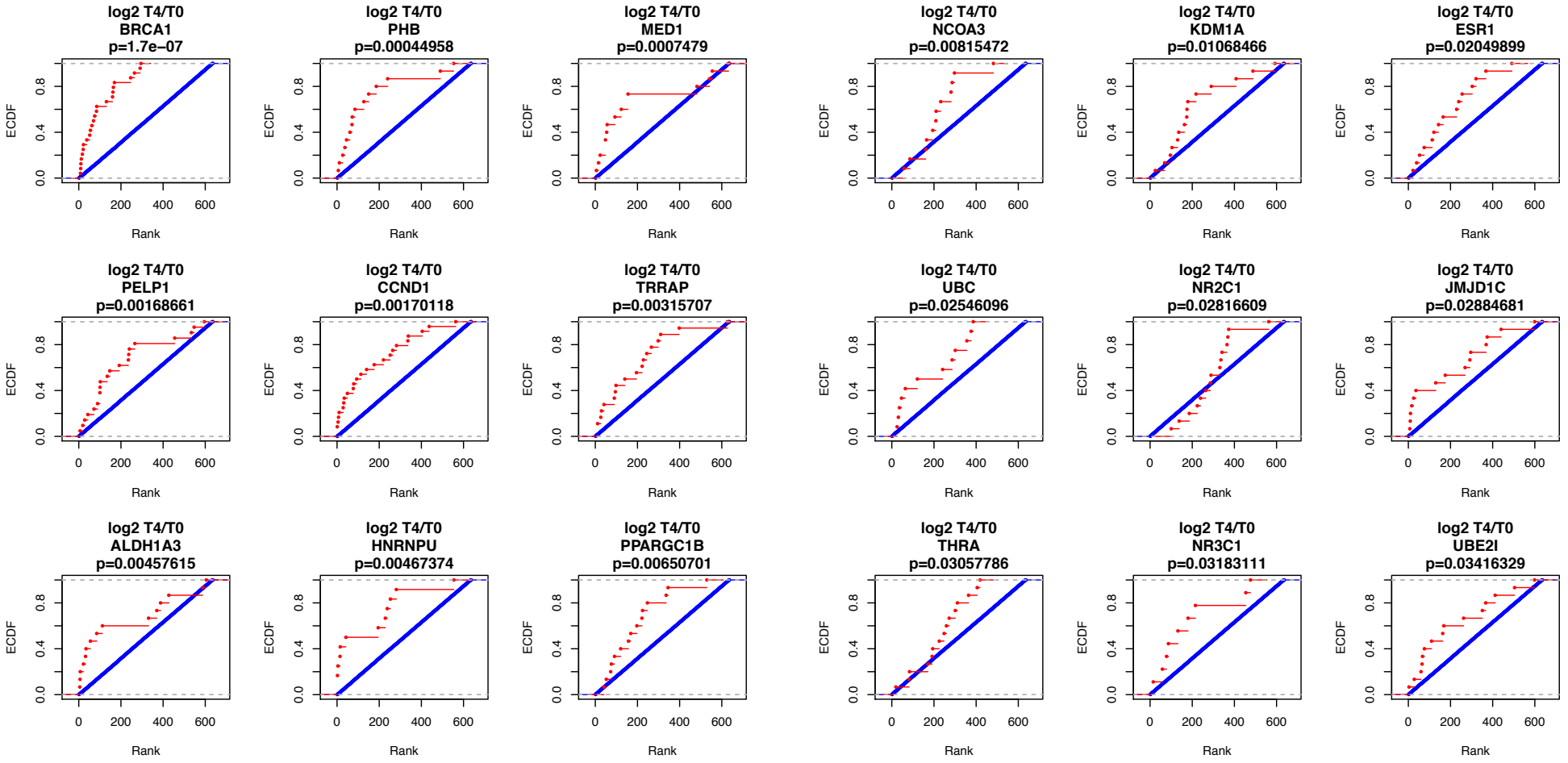

Supplementary Figure 3A - Page 2 of 8

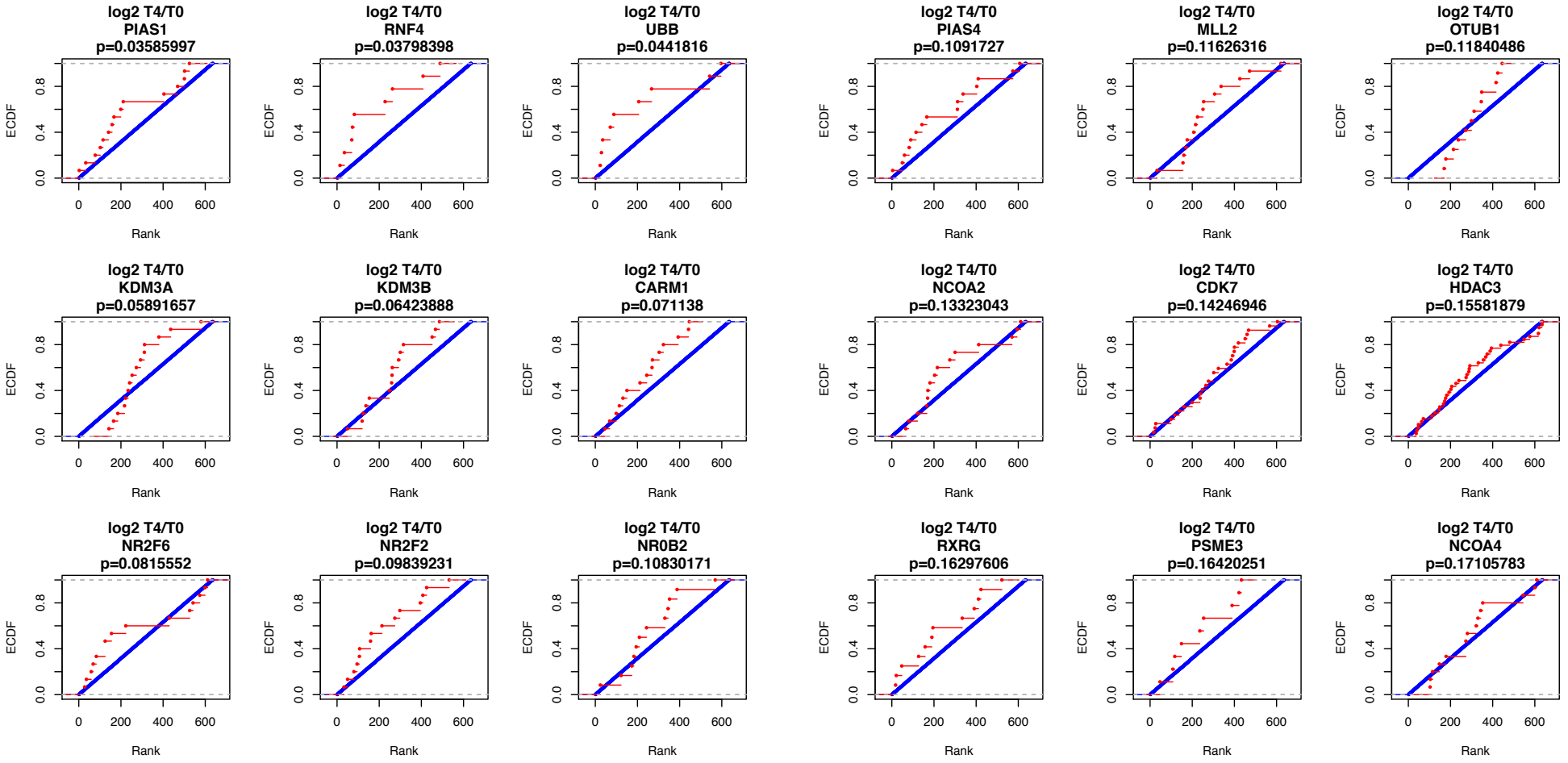

Supplementary Figure 3A - Page 3 of 8

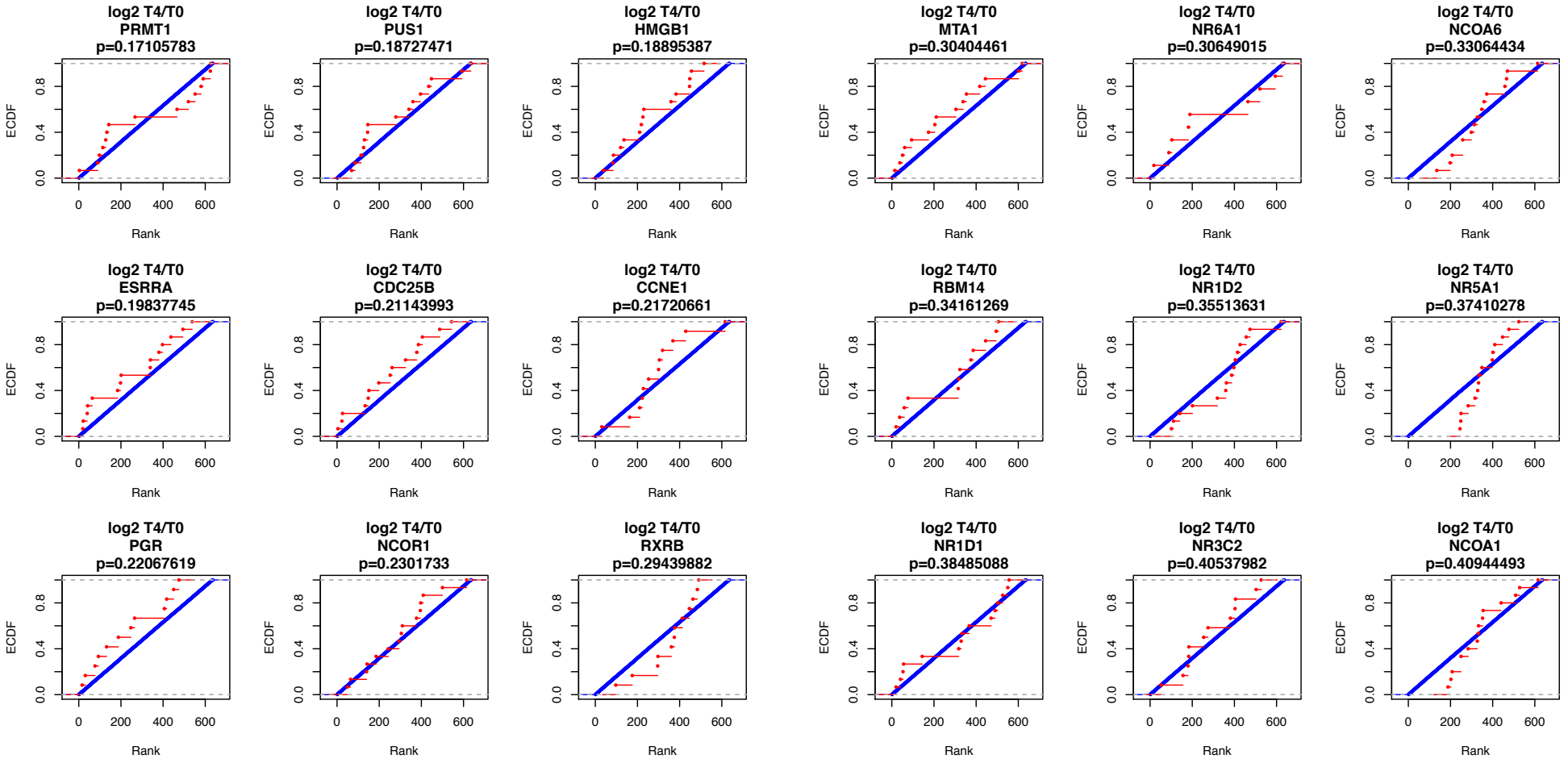

Supplementary Figure 3A - Page 4 of 8

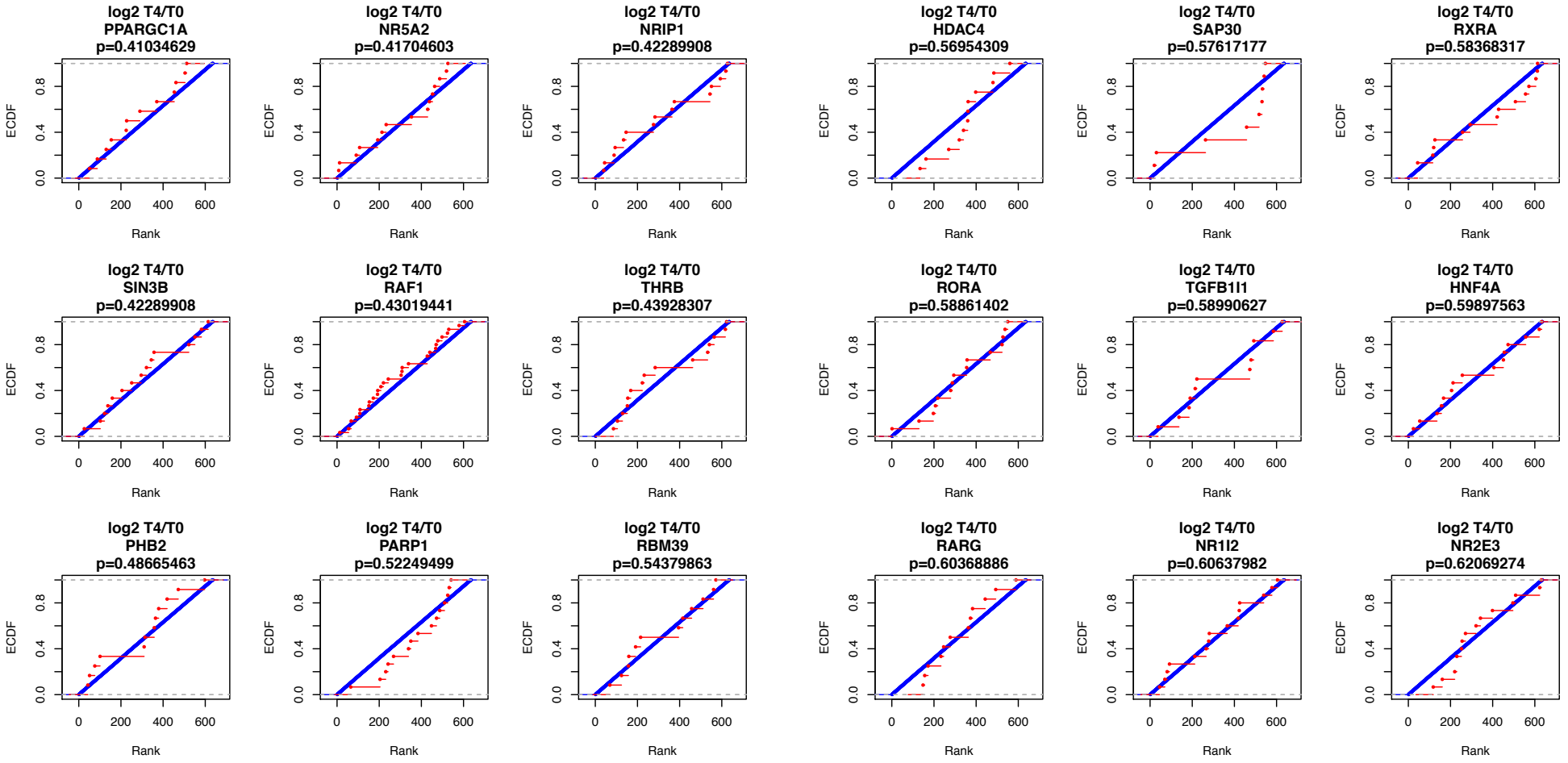

Supplementary Figure 3A - Page 5 of 8

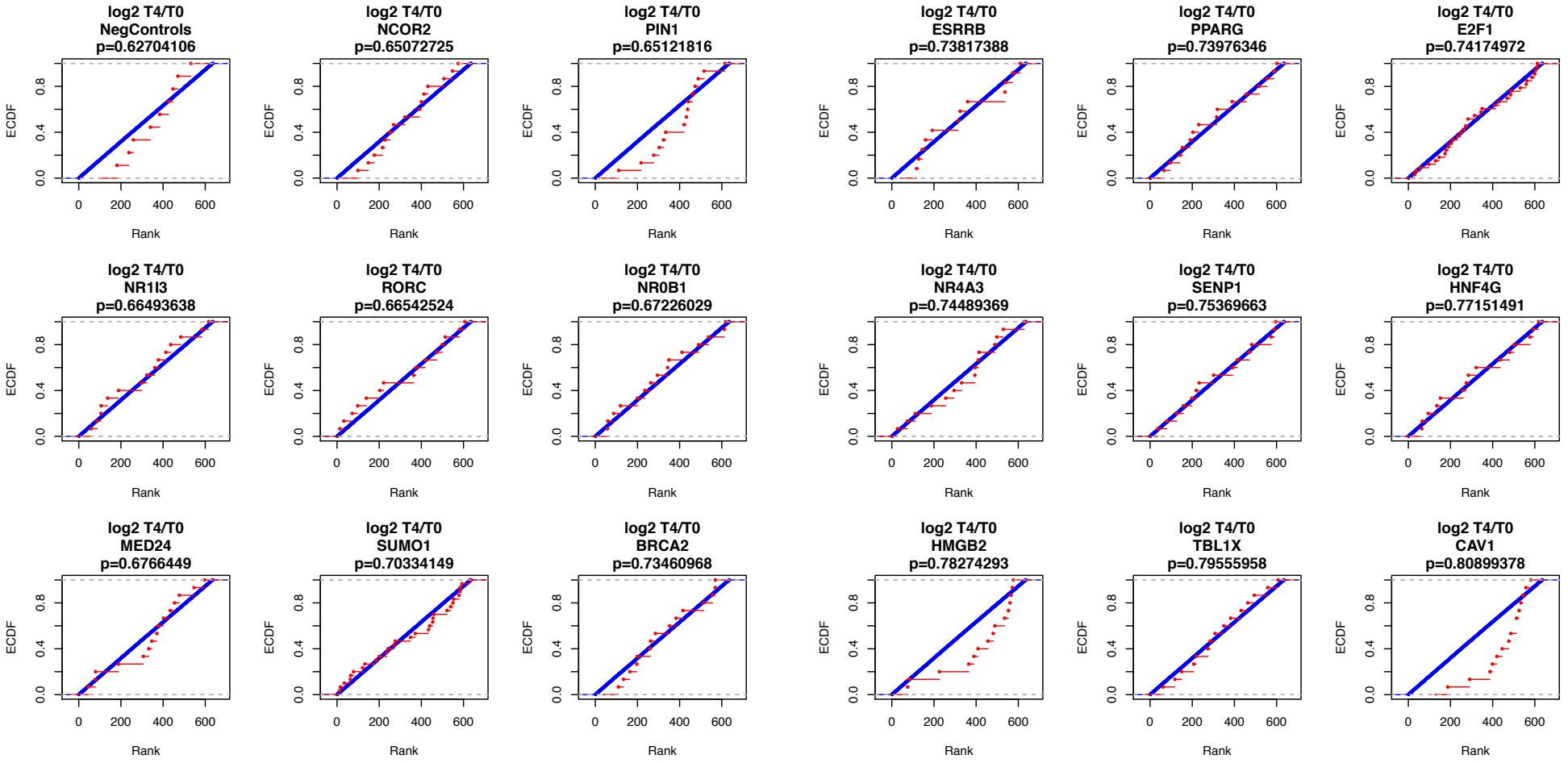

Supplementary Figure 3A - Page 6 of 8

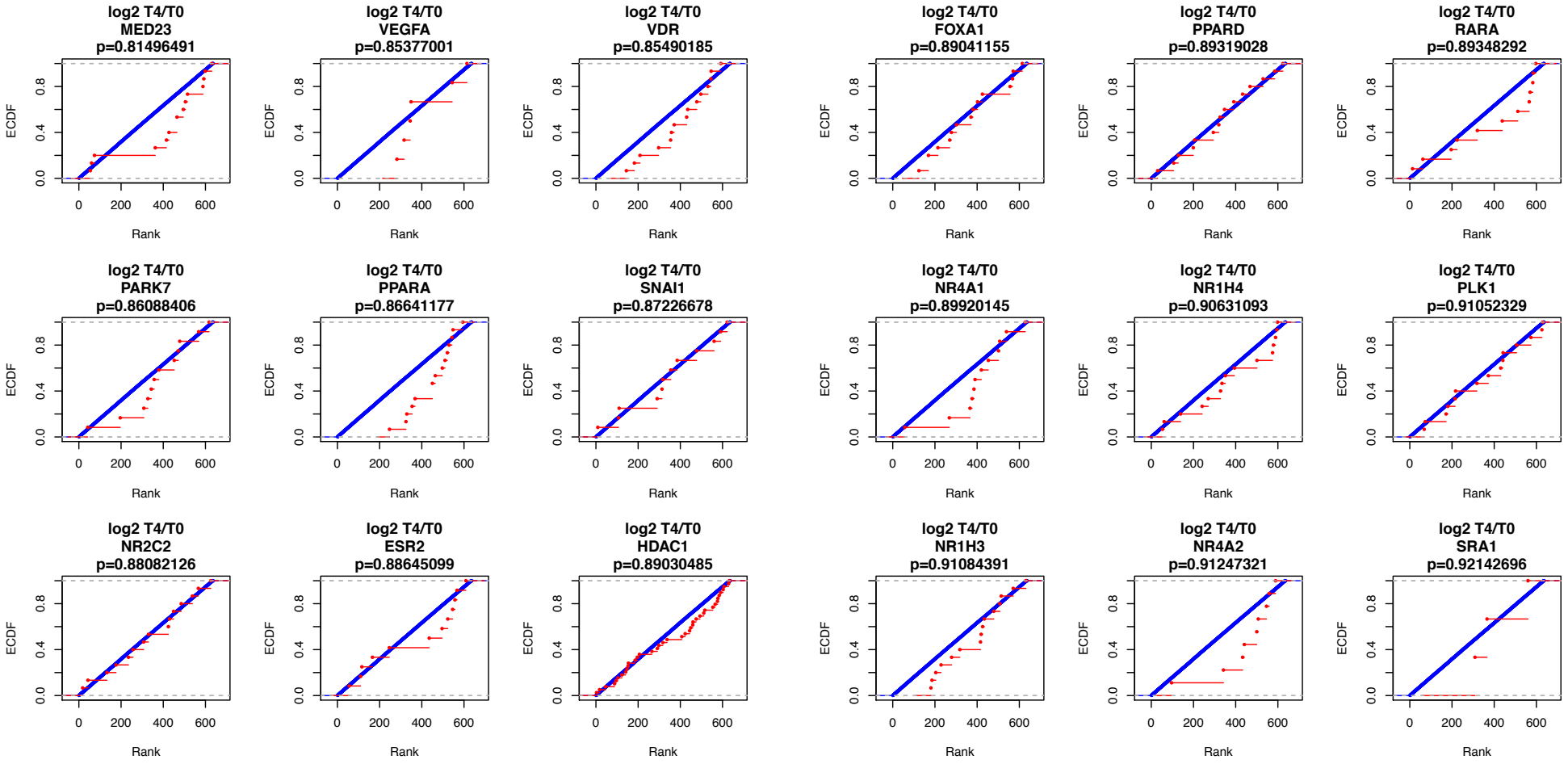

Supplementary Figure 3A - Page 7 of 8

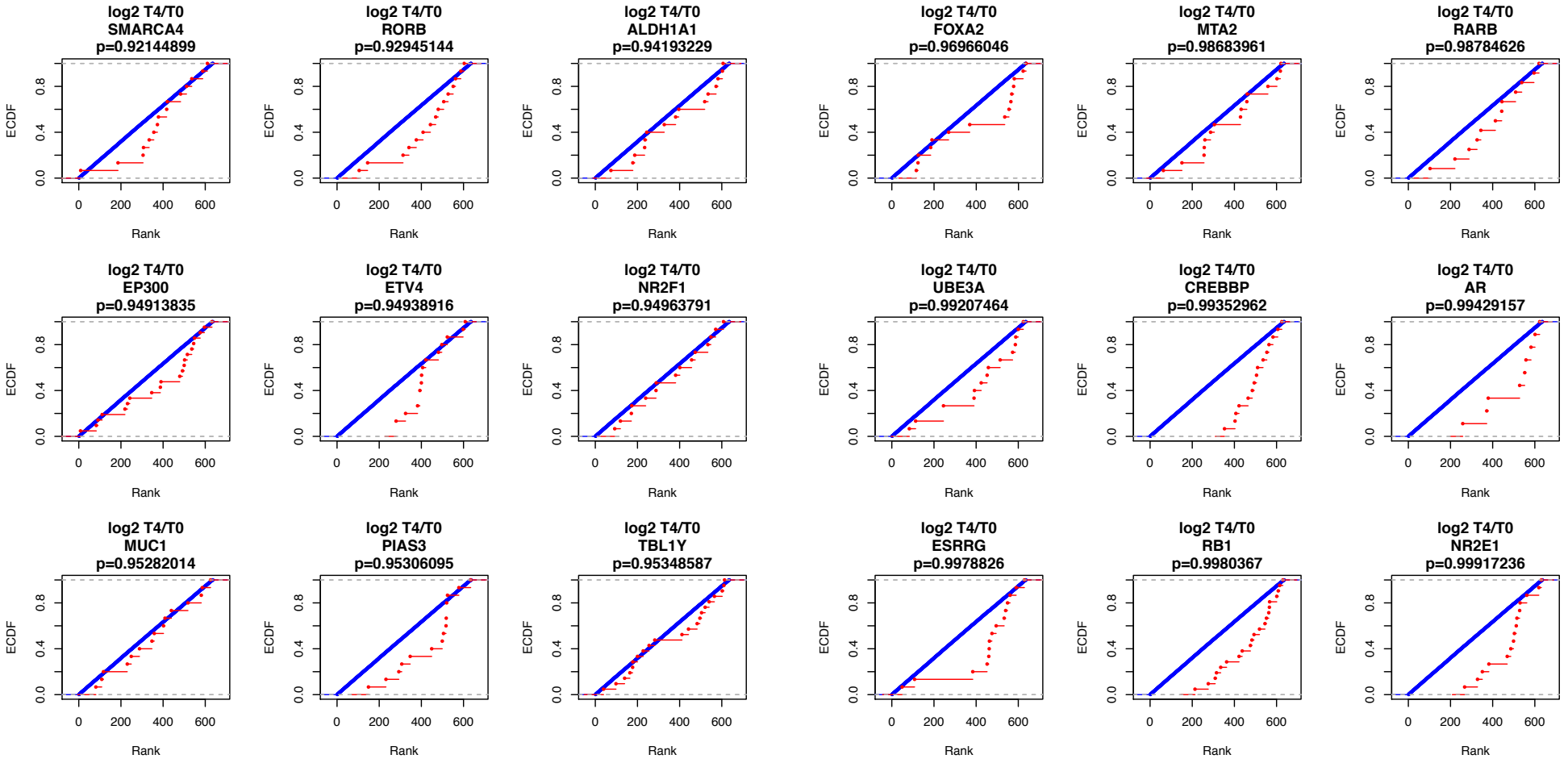

Supplementary Figure 3A - Page 8 of 8

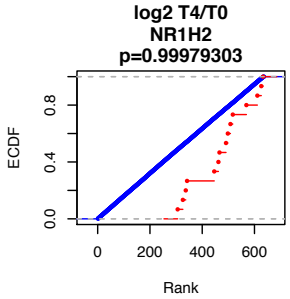

Figure S3A. Cumulative distribution function plots of rank-transformed shRNA abundance (log2 T4/T0) for each gene, compared to all other genes, *in vitro*. All replicates for individual shRNAs are shown in red, and all replicates for background shRNAs shown in blue.

Supplementary Figure 3B - Page 1 of 8

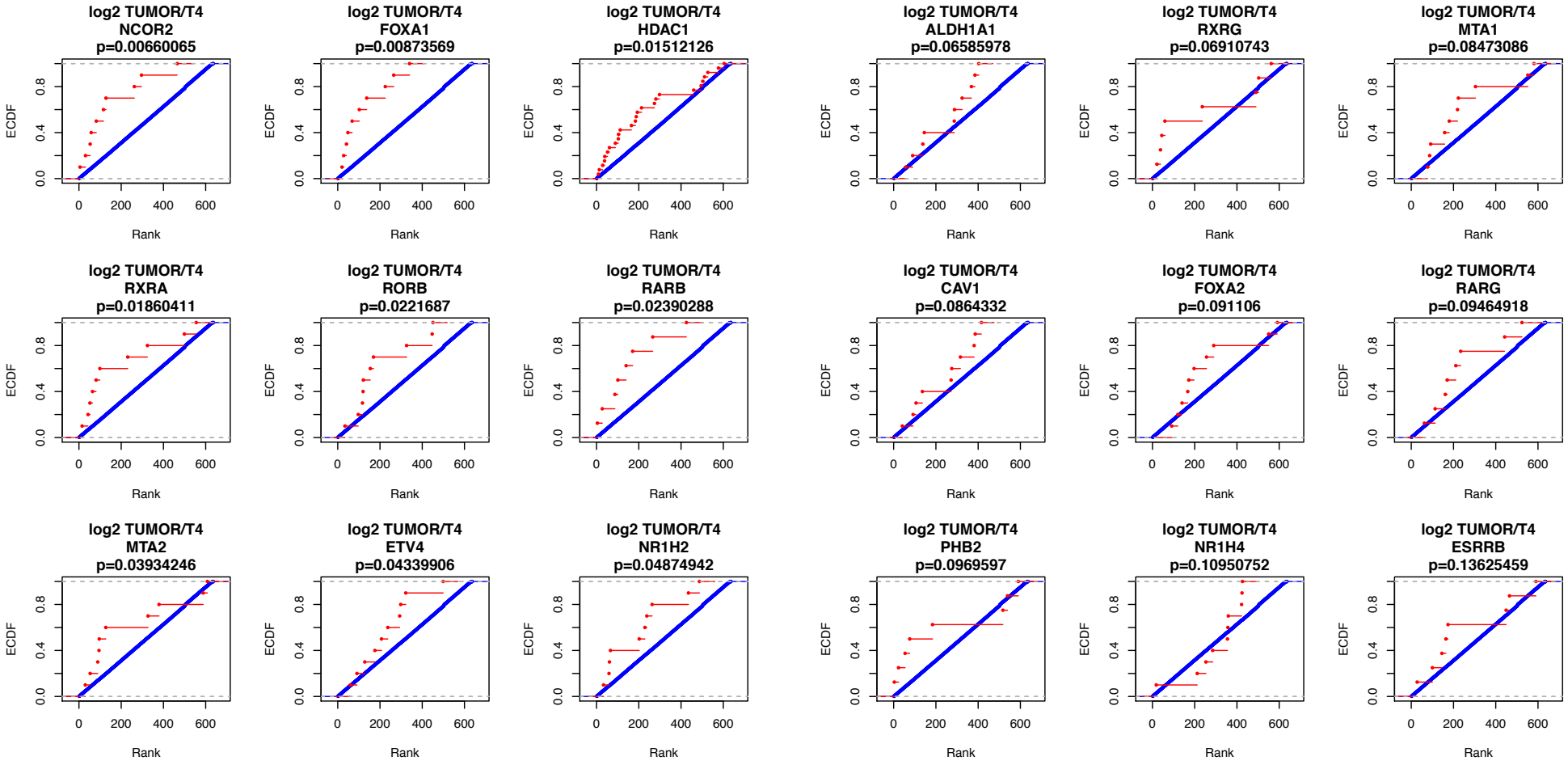

Supplementary Figure 3B - Page 2 of 8

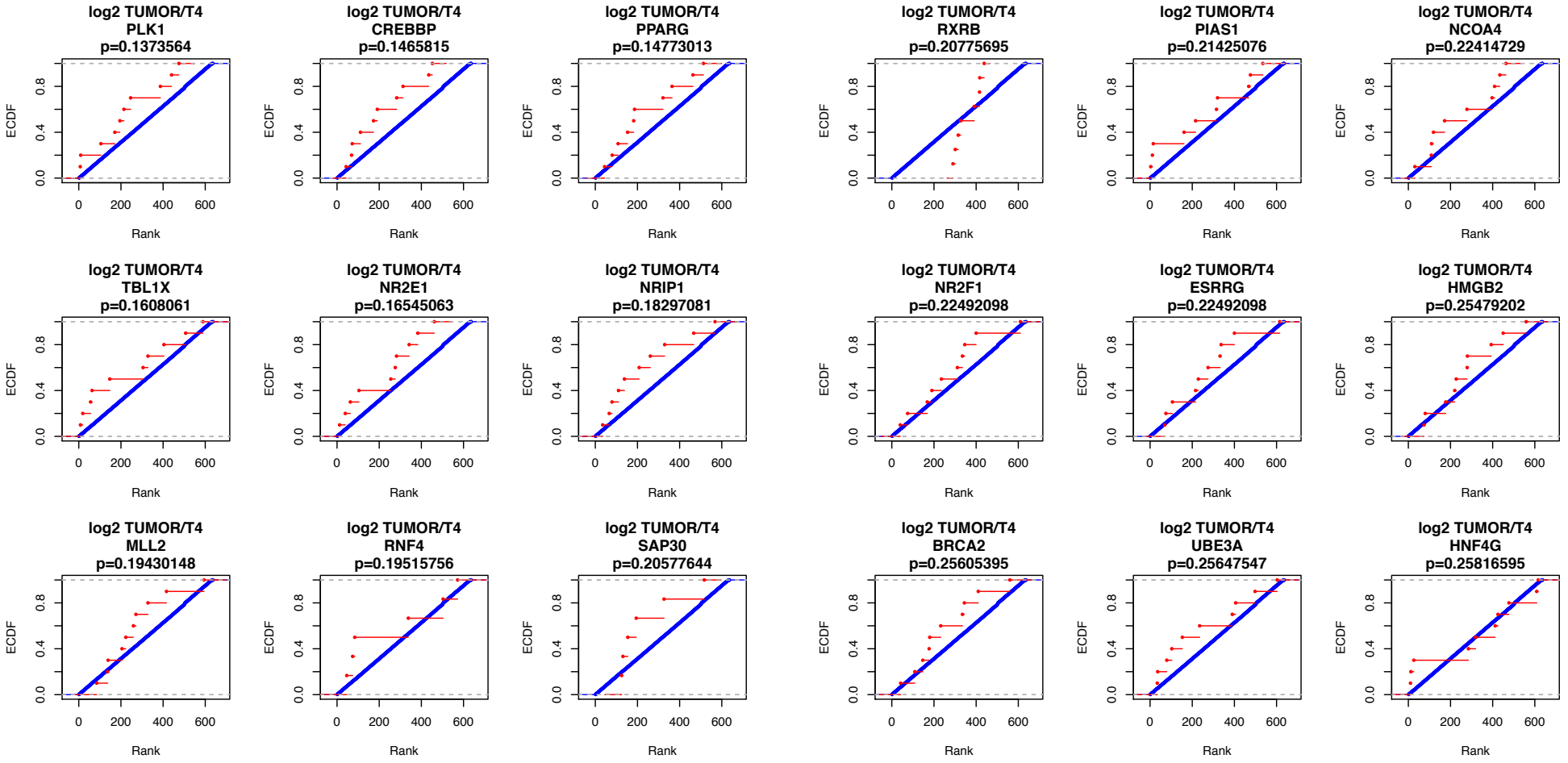

Supplementary Figure 3B - Page 3 of 8

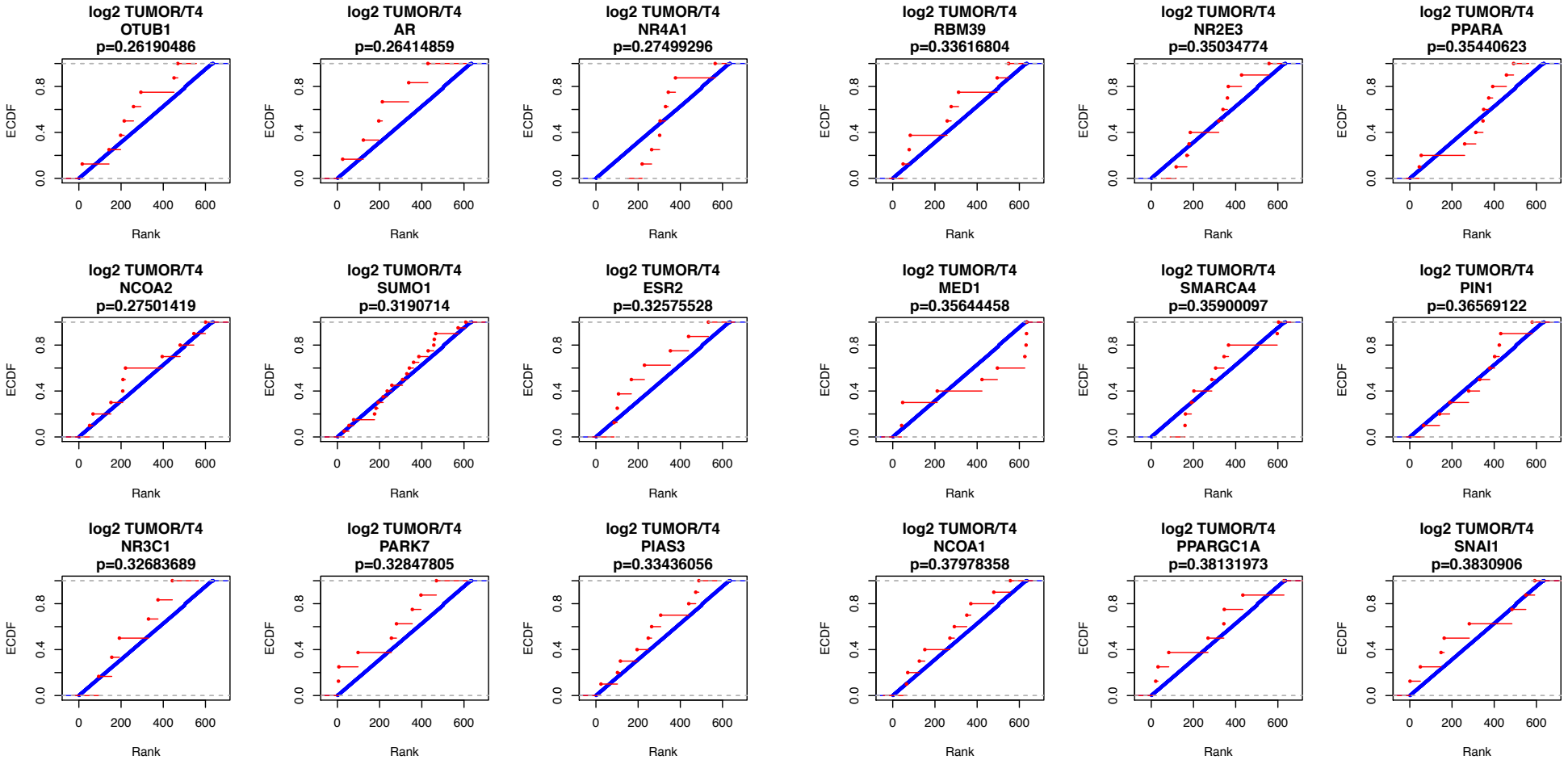

Supplementary Figure 3B - Page 4 of 8

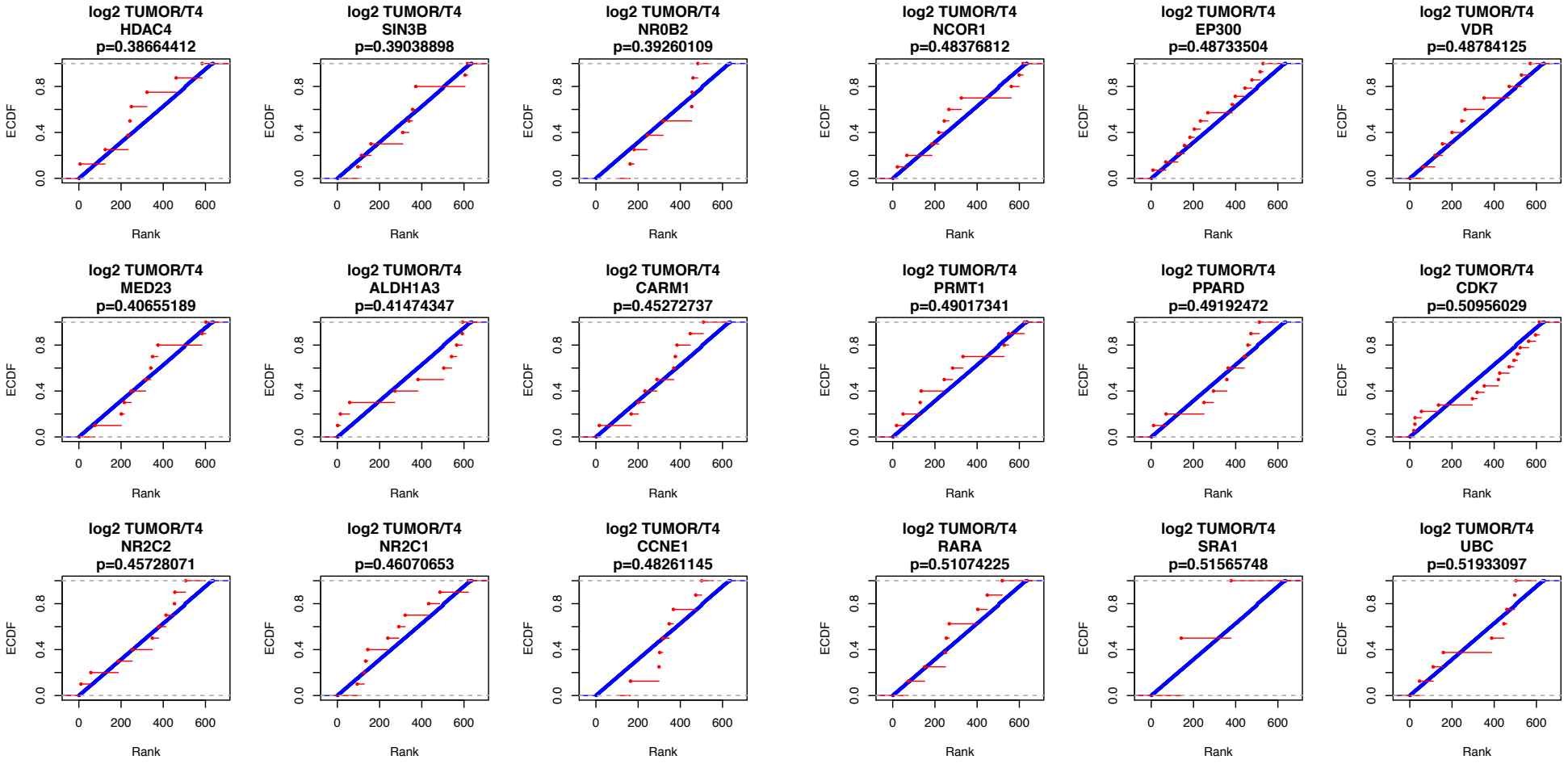

Supplementary Figure 3B - Page 5 of 8

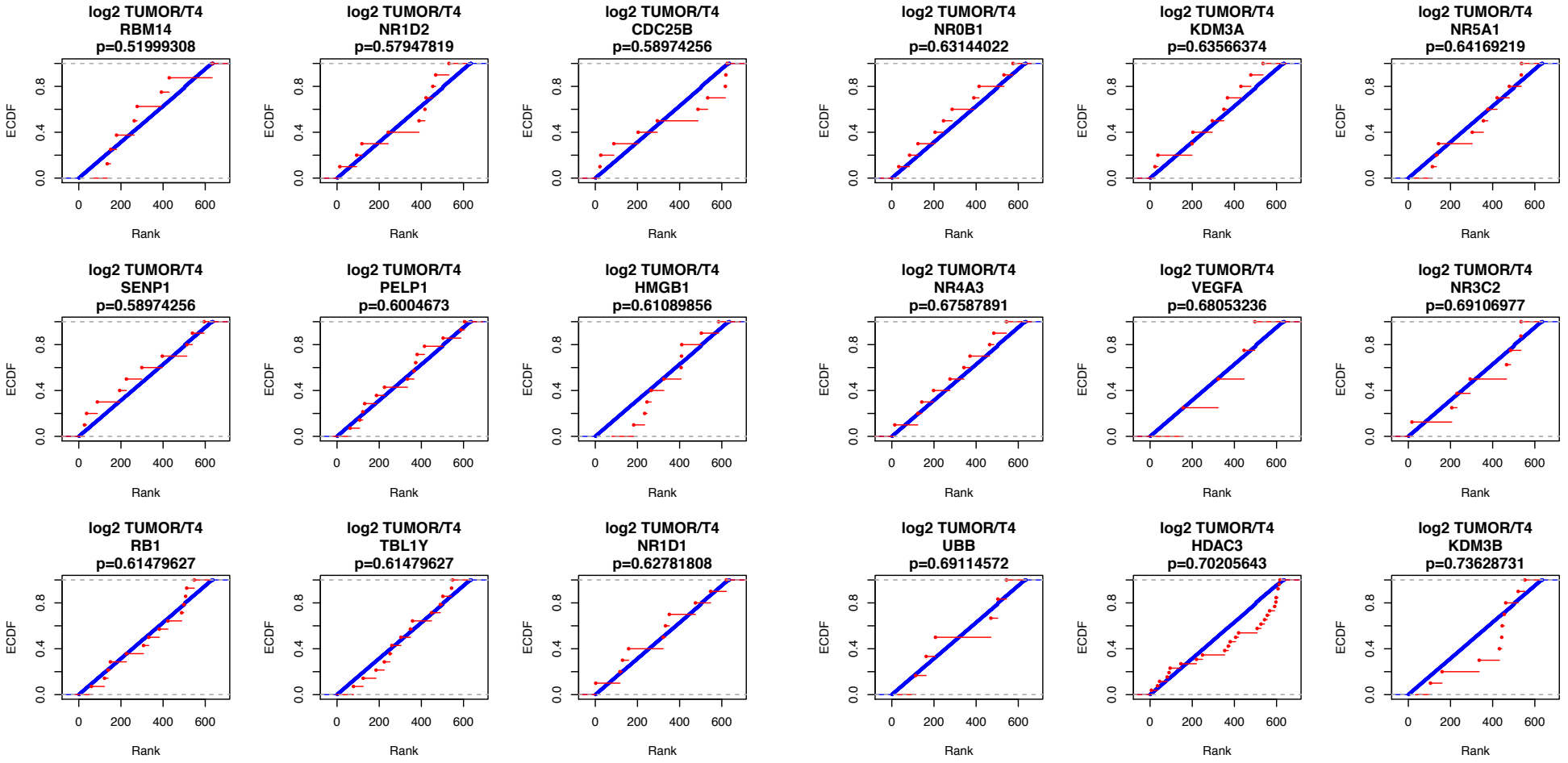

Supplementary Figure 3B - Page 6 of 8

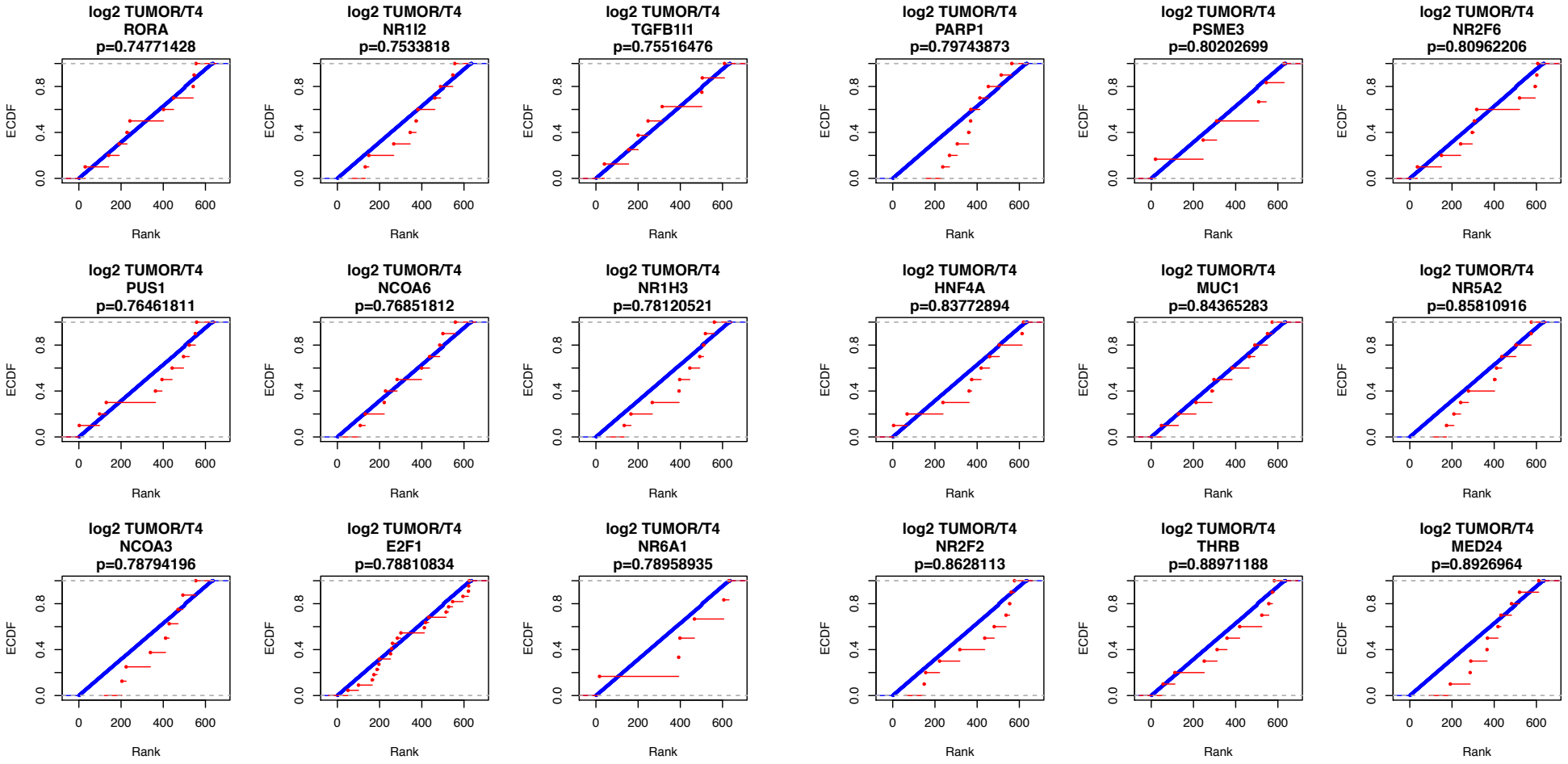

Supplementary Figure 3B - Page 7 of 8

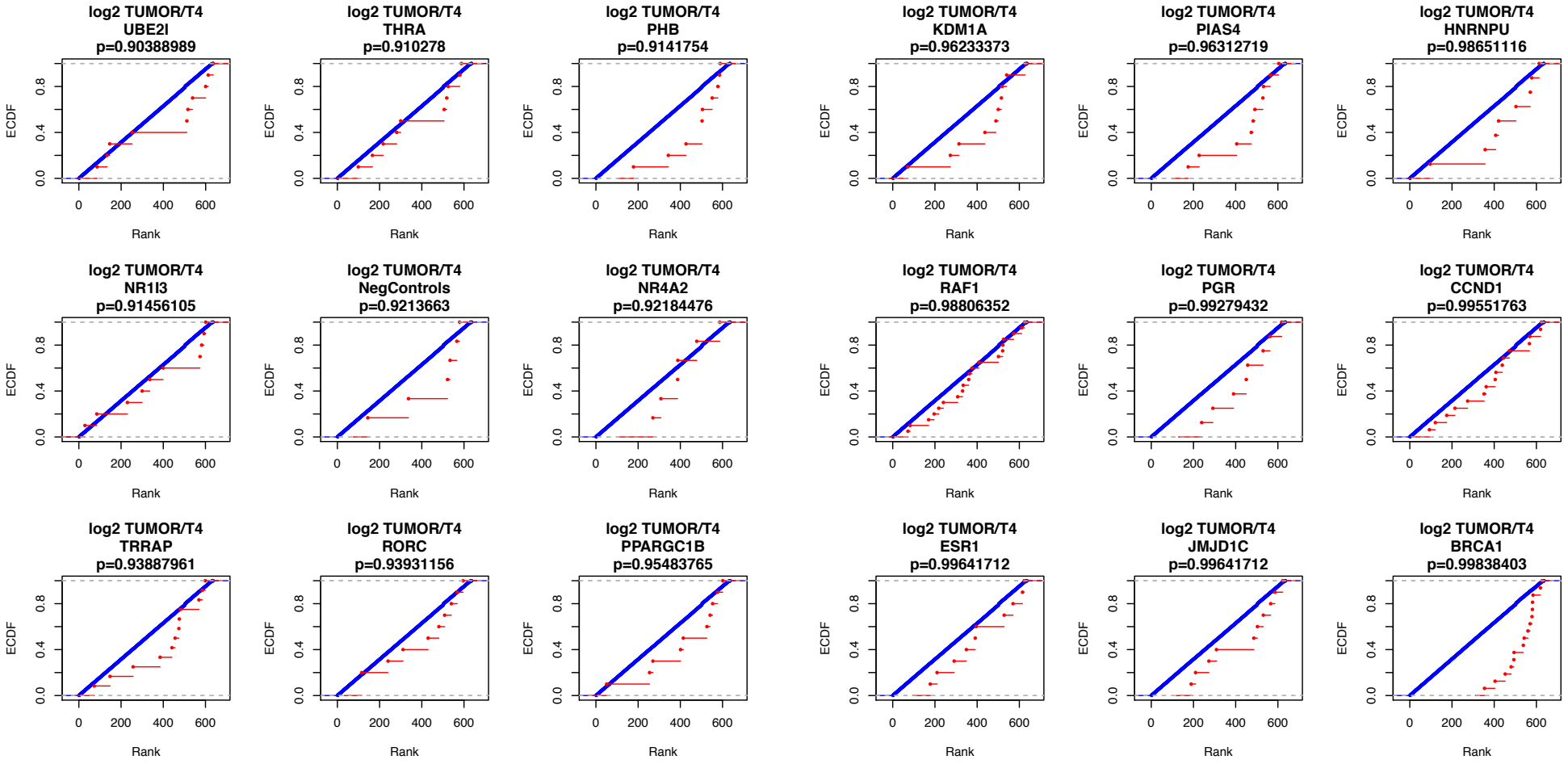

Supplementary Figure 3B - Page 8 of 8

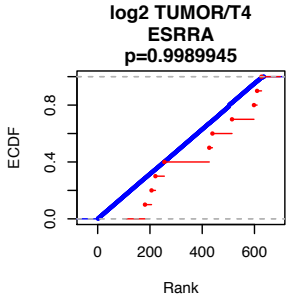

Figure S3B. Cumulative distribution function plots of rank-transformed shRNA abundance (log2 tumor/T4) for each gene, compared to all other genes, *in vivo*. All replicates for individual shRNAs are shown in red, and all replicates for background shRNAs shown in blue.

Supplementary Figure 4

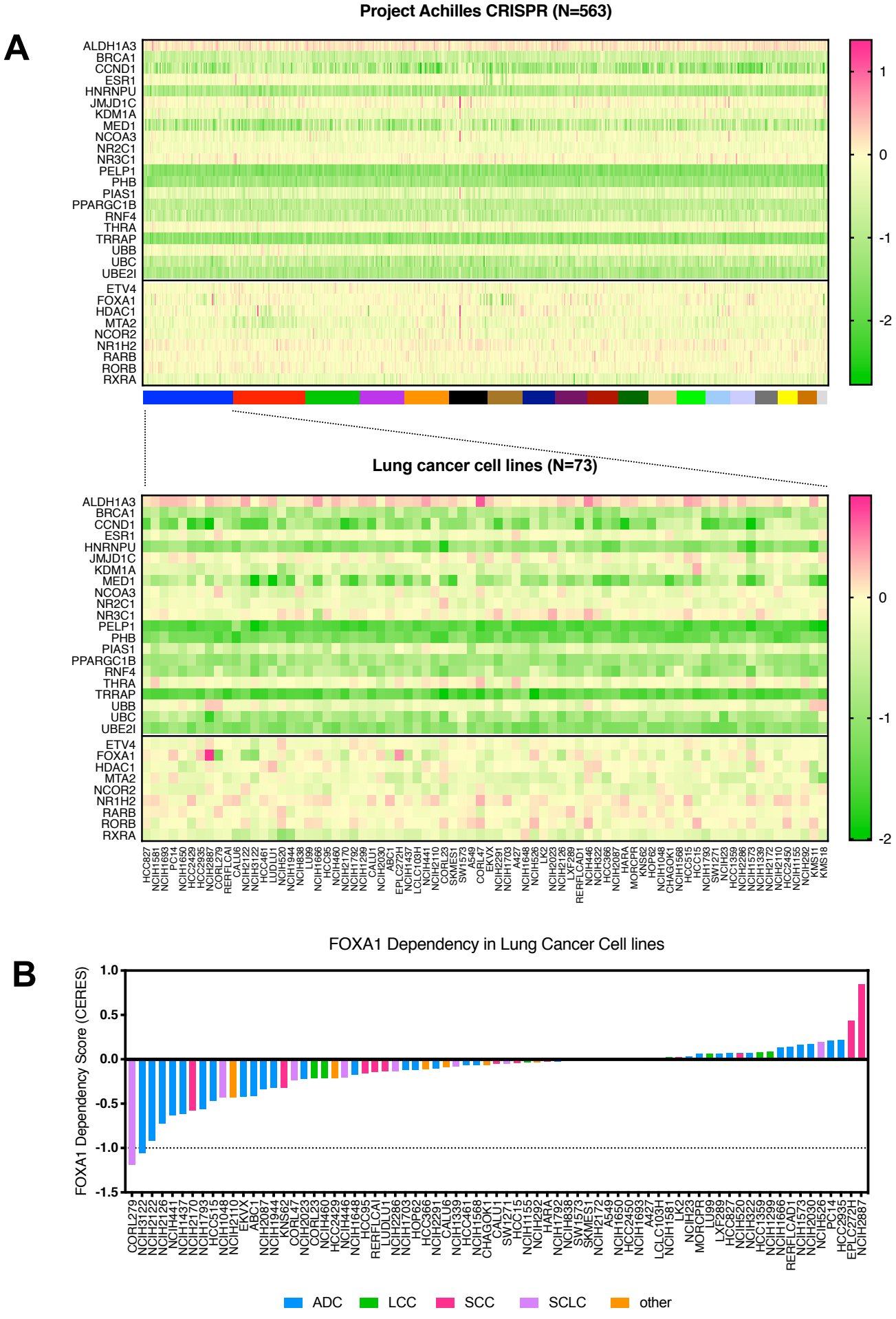

Figure S4. Analysis of shRNA screen hits in Project Achilles CRISPR datasets. (A) CERES scores from *in vitro* dropout screens performed with the CRISPR Avana library (Project Achilles/DepMap Consortium) for 30 Nuclear Receptor/Co-Regulator genes which showed significant dropout in the shRNA screen described here. Genes with significant dropout *in vitro* are indicated above the horizontal black line, and genes showing preferential dropout *in vivo* are below. Top panel, CERES scores in 563 human cancer lines. Lineages are indicated by different colors in the horiztonal color bar. Bottom panel, CERES scores in 73 lung cancer lines. (B) CERES scores for FOXA1 dependency across lung cancer cell lines. All data was obtained through the public DepMap portal (https://depmap.org/).

Supplementary Figure 5

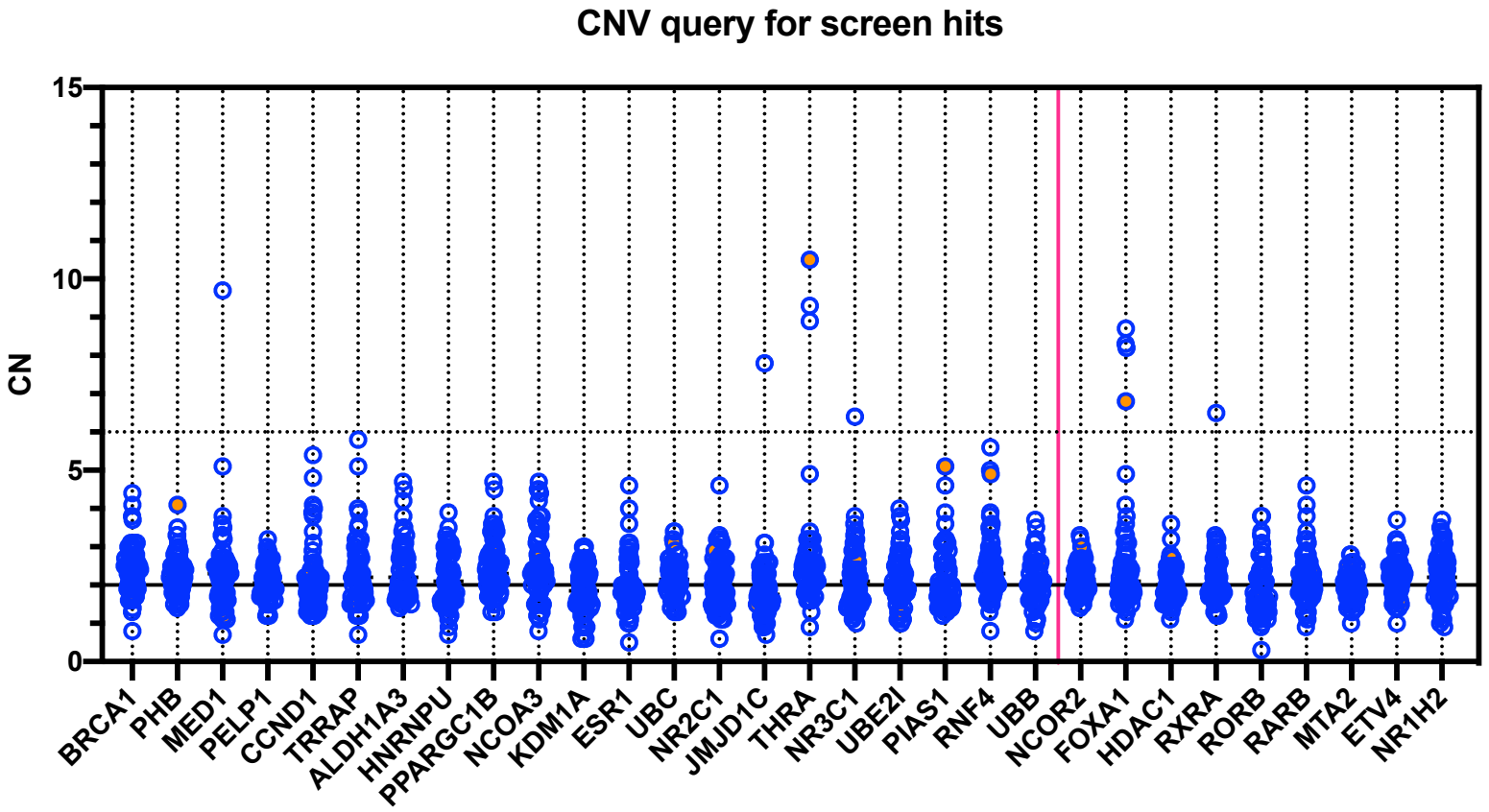

Figure S5. Copy number analysis of shRNA screen hits in NSCLC cell lines. Analysis of high resolution SNP array profiling across a panel of NSCLC cell lines (N = 63). Candidate genes from the *in vitro* screen are shown to the left of the red line, and candidates from the *in vivo* screen are shown to the right. H1819 is indicated by orange points.

Supplementary Figure 6

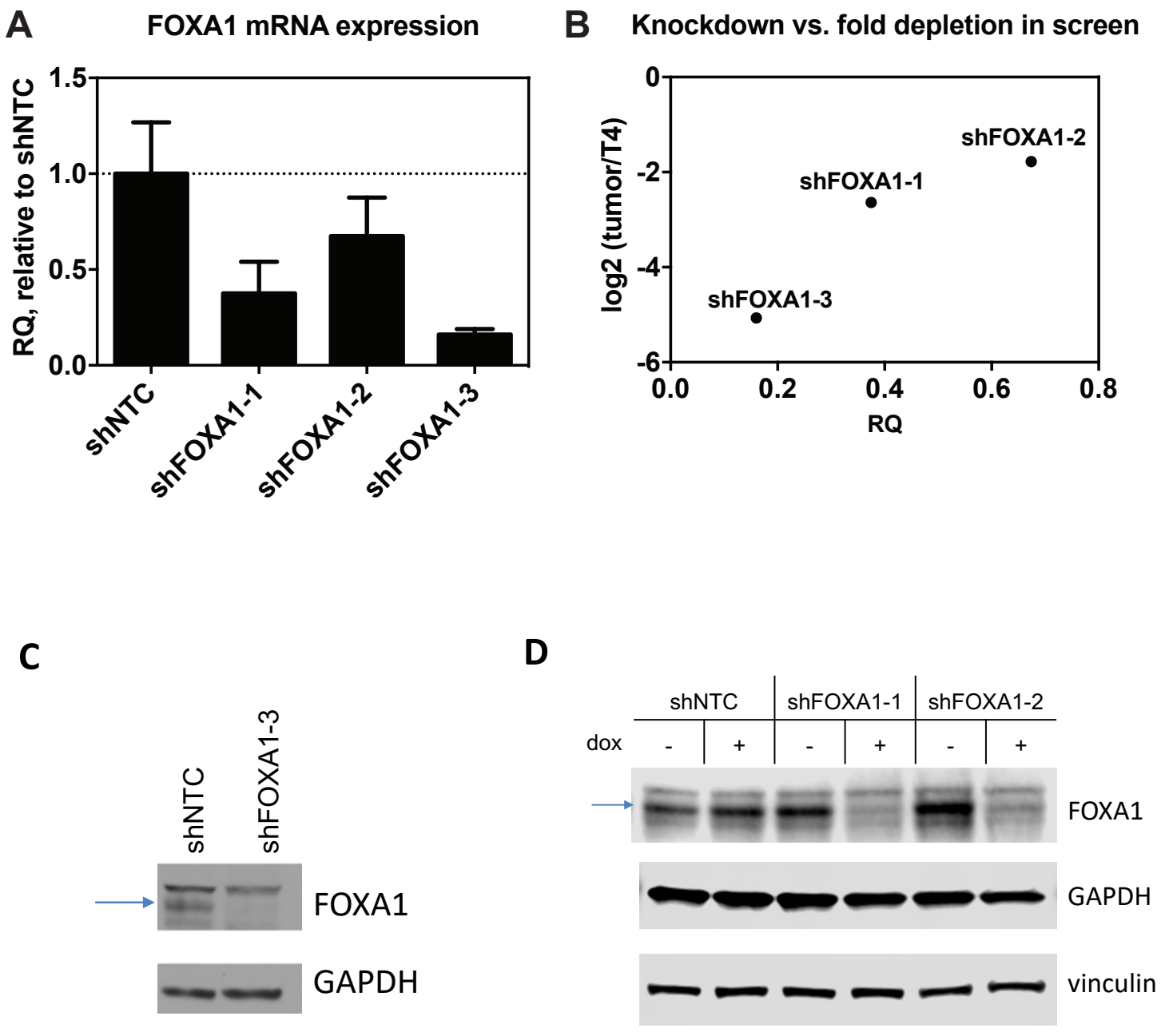

Figure S6. Knockdown of FOXA1 with individual short hairpins correlates with function in the screen. (A) Three short hairpins against FOXA1 exhibit varying ability to knockdown their target as assessed by QPCR for FOXA1 mRNA. (B) Level of knockdown as measured by Q-RTPCR correlates with the level of depletion observed for each shRNA in the screen. (C) Western blot showing knockdown of FOXA1 at the protein level with shFOXA1-3. (D) Western blot showing knockdown of FOXA1 in H1819 using two dox-inducible shRNAs against FOXA1.

Supplementary Figure 7

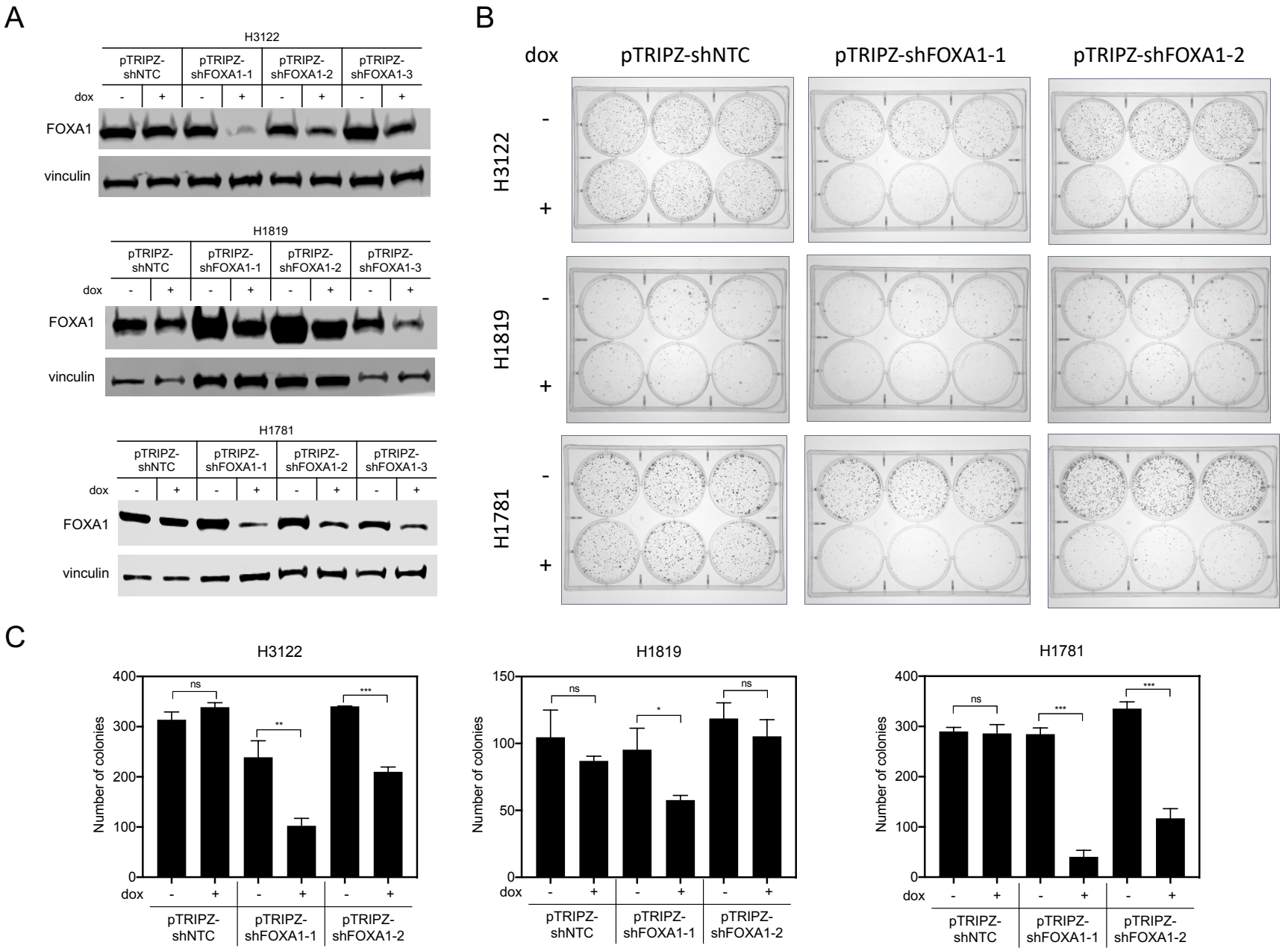

Figure S7. Confirmation of FOXA1 shRNA specificity using dox-inducible shRNA constructs. (A) Western blots showing knockdown of FOXA1 with three different pTRIPZ-shFOXA1 constructs in FOXA1-amplified cell lines. Lysates were prepared by directly lysing into 4x SDS-Loading Buffer. We speculate that multiple bands observed in samples lysed in lysis buffer (Figure 3; Supplementary Figure 6) may be due to post-translational modifications – or other non-specific antigens - that do not survive harsher lysis conditions. (B) Colony formation assays in FOXA1-amplified cell lines with two different pTRIPZ-shFOXA1 constructs. (C) Quantification of colony formation assays. P-values were calculated using one-sided t-tests (alpha=0.05).

Supplementary Figure 8

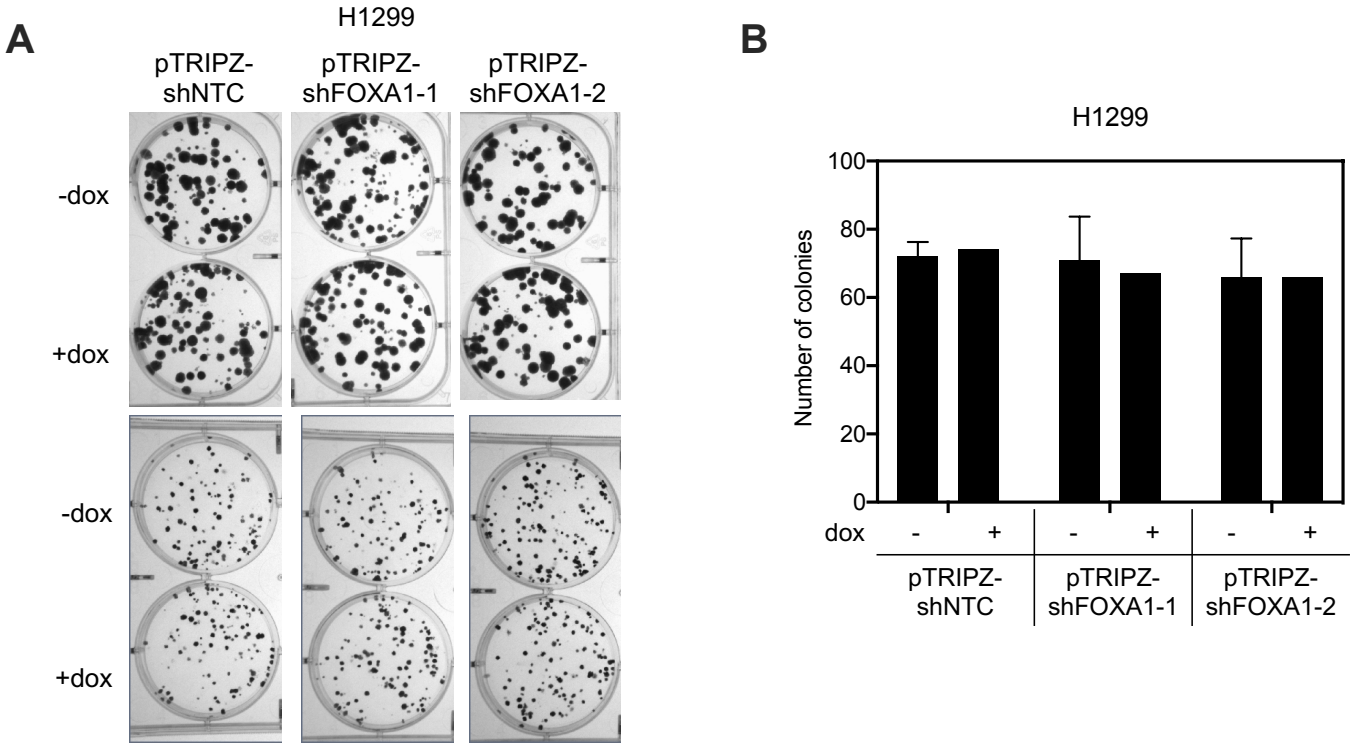

Figure S8. Confirmation of FOXA1 shRNA specificity using dox-inducible shRNA constructs in a FOXA1-negative cell line. (A) Colony formation assays in a FOXA1-negative cell line with two different pTRIPZ-shFOXA1 constructs. Top panel, 125 cells were seeded per well, and the assay was terminated after ~10 days. Bottom panel, 75 cells were seeded per well, and the assay was terminated after ~7 days. (B) Quantification of colony formation assays. P-values were calculated using one-sided t-tests (alpha=0.05).

Supplementary Figure 9

A

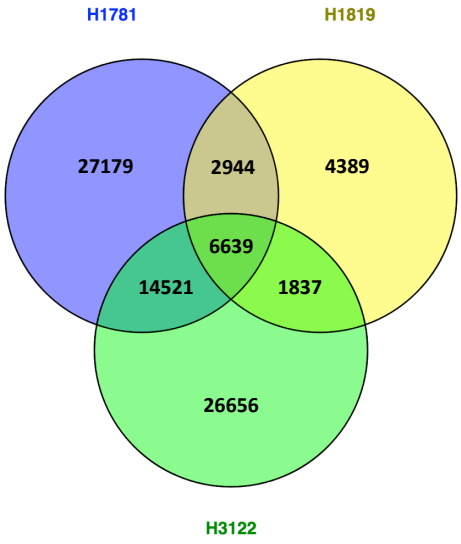

Cell line	Total peaks	% of total peaks common to all three cell lines
H1819	15809	42%
H1781	51283	13%
H3122	49553	13%

B

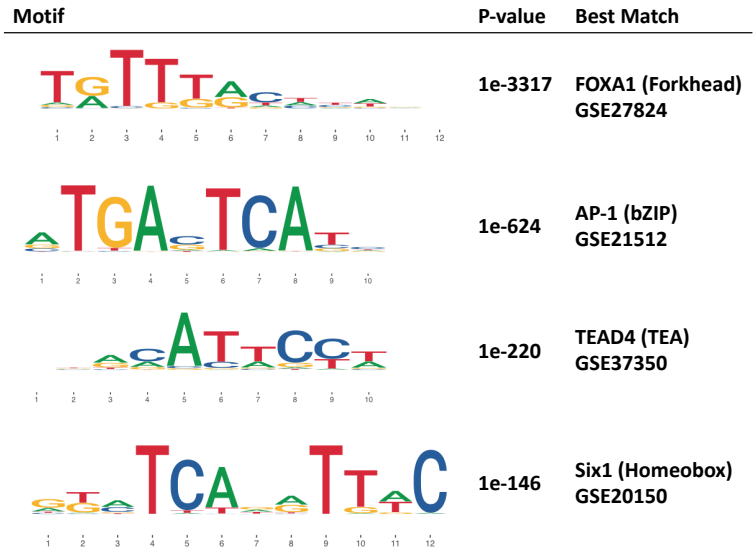

C

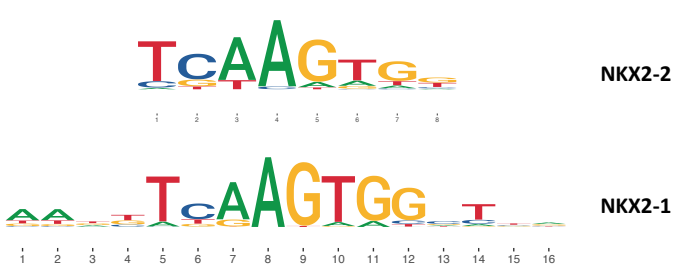

Figure S9. Characterization of FOXA1 genomic binding sites. (A) Venn diagram illustrating the overlap between FOXA1 peak midpoints in H1819, H1781, and H3122. (B) Top 4 most significant primary motifs found to be enriched in FOXA1-bound regions. (C) Comparison of NKX2-2 consensus motif (JASPAR ID: PH0111.1) with NKX2-1 consensus motif (JASPAR ID: PH0171.1).

Supplementary Figure 10

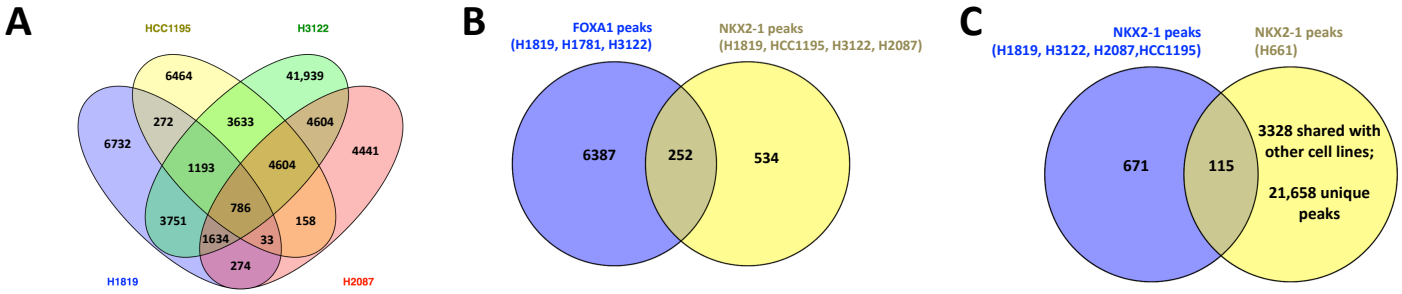

Figure S10. Comparison of the FOXA1 cistrome to the NKX2-1 cistrome in NSCLC cell lines harboring 14q amplification. Venn diagrams illustrating (A) the overlap between NKX2-1-bound genomic regions in H1819, H3122, H2087, and HCC1195; (B) the overlap between FOXA1-bound genomic regions and NKX2-1-bound genomic regions; (C) the overlap between NKX2-1 peaks shared among all four co-amplified cell lines with 1 cell line with focal amplification of NKX2-1: H661.

Supplementary Figure 11

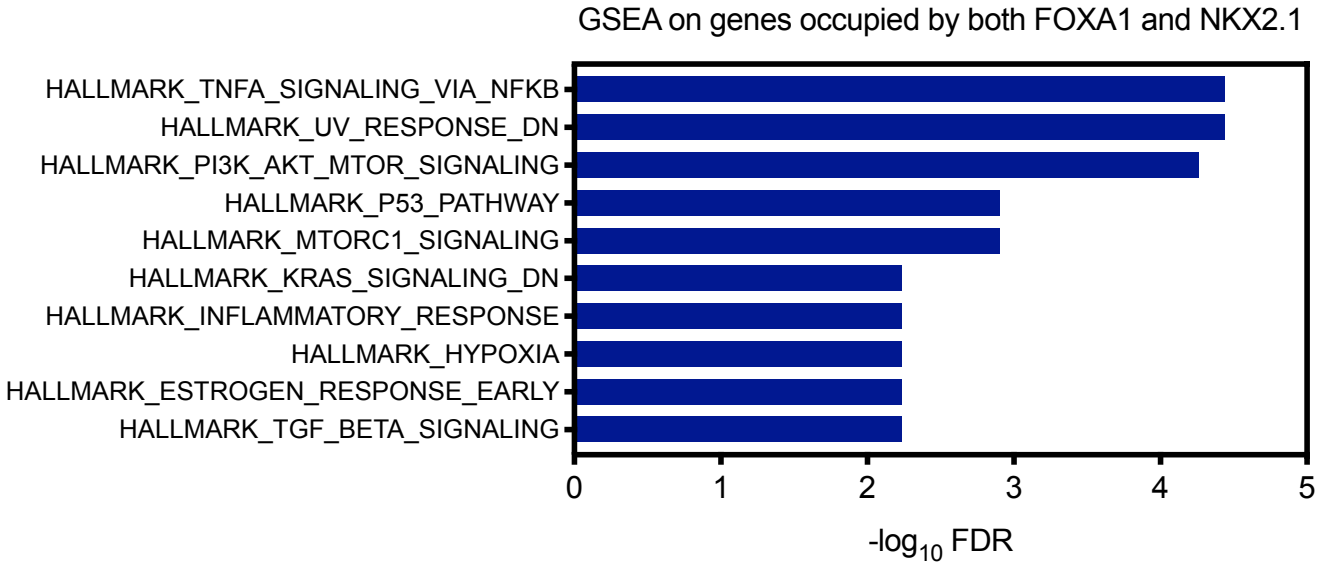

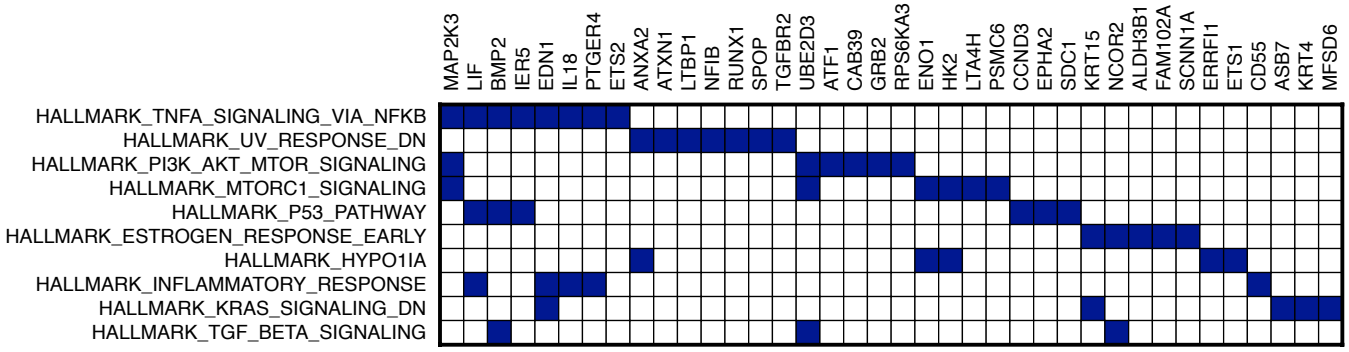

Figure S11. Gene set enrichment analysis among genes with TSS within 10 kb of genomic regions occupied by both FOXA1 and NKX2-1. Top panel: Top 10 MSigDB Hallmark gene sets that are significantly enriched in the gene list. Bottom panel: Gene membership in the sets listed above.

Supplementary Figure 12

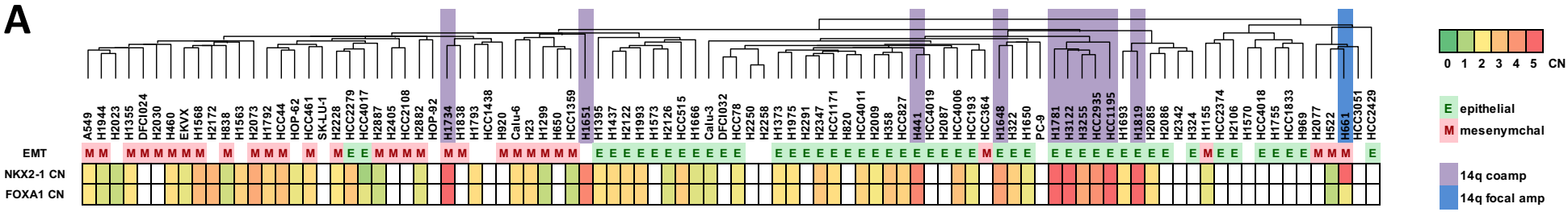

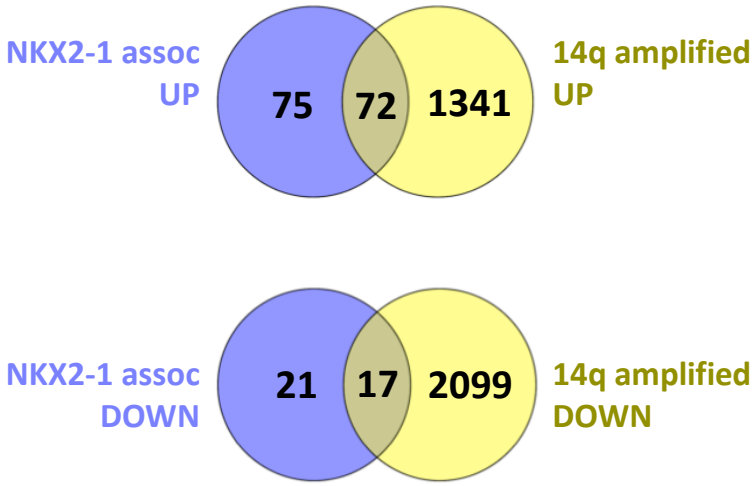

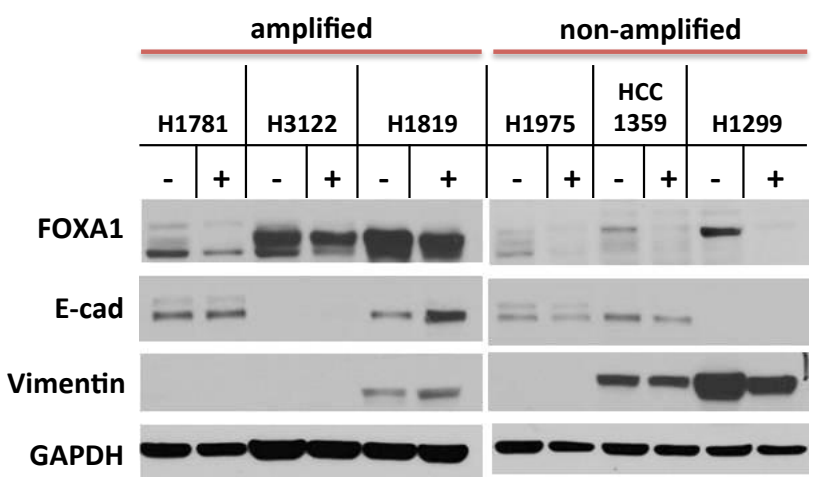

Figure S12. NSCLCs harboring 14q-amplification are a molecularly distinct subset from other lung tumors. (A) Unsupervised clustering of genome-wide expression profiles of 94 NSCLC lung cancer cell lines. Cell lines highlighted in purple harbor 14q amplification ≥ 4 that spans both the *FOXA1* and *NKX2-1* locus. Cell lines highlighted in blue harbor 14q amplification that spans only *NKX2-1*. Epithelial or mesenchymal status as determined by protein expression of e-cadherin and vimentin is indicated by 'E' or 'M', respectively. (B) Venn diagrams showing overlap of upregulated genes (top) or downregulated genes (bottom) with a previously published list of NKX2-1 associated genes. (C) Western blotting for E-cadherin and vimentin with and without knockdown of FOXA1 in a panel of cell lines representing high (amplified) or low (non-amplified) FOXA1 copy number.

Supplementary Figure 13

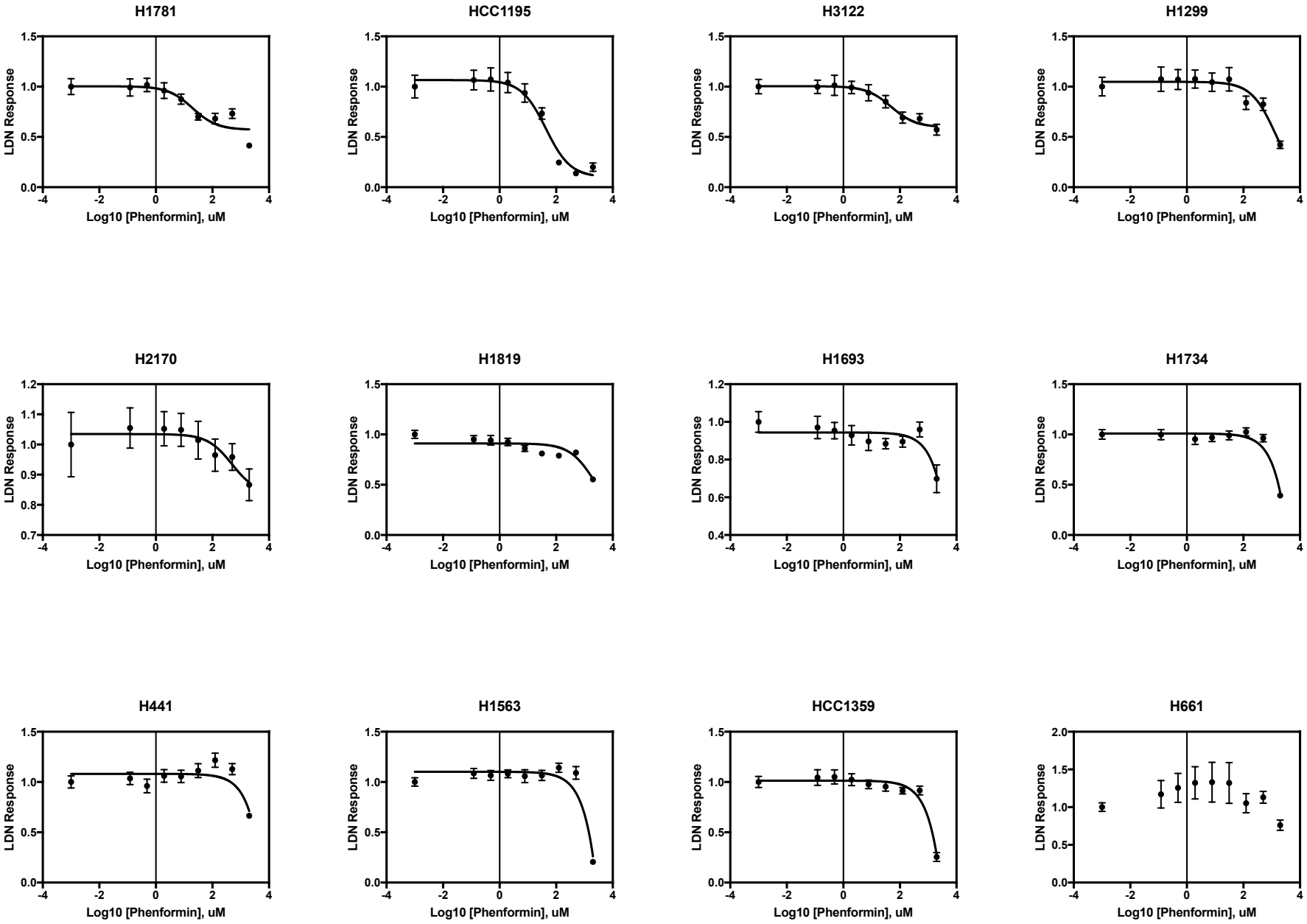

Figure S13. Dose response curves to phenformin in a panel of NSCLC cell lines. Cell viability was measured via MTS assay, and is reported as the low-dose normalized response. Points shown are the average of 8 technical replicates, and error bars represent the error-propagated standard deviation. Red arrows indicate outlier datapoints that were omitted when calculating IC50s.

Table S1. Gene coverage in shRNA library used in this study.

Table S2. Primers used to amplify and quantify shRNA sequences.

Table S3. Log_2 fold changes in shRNA abundance in the shRNA screen.

Table S4. P-values from KS-tests for each gene represented in the screen.

Table S5. Locations of common FOXA1 peaks in H1819, H1781, H3122.

Table S6. Locations of common NKX2-1 peaks in H1819, HCC1195, H3122, and H2087.

Table S7. Nearest genes to genomic regions with both FOXA1 and NKX2-1 binding.

Table S8. Overlap statistics for genomic regions occupied by NKX2-1 in H1910, HCC1195, H3122, H2087, and H661.

Table S9. NSCLC cell lines from the UTSW cohort, listed with histotype and FOXA1 and NKX2-1 copy number levels (SNP CNV).

Table S10. Differentially expressed genes between NSCLC cell lines with co-amplification of FOXA1 with NKX2-1 and cell lines with normal FOXA1 and NKX2-1 copy number.

Table S11. Primary LUAD from the SPORE dataset, listed with histotype and FOXA1 and NKX2-1 copy number levels (aCGH).

Table S12. Differentially expressed genes between primary LUAD with co-amplification of FOXA1 with NKX2-1 and LUAD with normal FOXA1 and NKX2-1 copy number.

Table S13. Differentially expressed genes in H1781 after knockdown of FOXA1. RNA-seq based expression profiling on RNA from two replicate knockdown experiments in lung adenocarcinoma line NCI-H1781 identified 5,363 genes which were differentially expressed after knockdown of FOXA1 (FDR<5%).

Table S14. Differentially expressed genes in H1819 after knockdown of FOXA1. Expression profiling in H1819 cells after knockdown of FOXA1 revealed that the dynamic range of gene expression after knockdown was significantly smaller in H1819 than H1781, which may be attributed to lower FOXA1 copy number in this cell line. An FDR cutoff of 5% did not identify any genes as differentially expressed in H1819, however a less stringent statistical filter identified 179 DEG ($p<0.01$, 2-sample t-test).

Table S15. Phenformin IC50s across a panel of NSCLC cell lines.

Table S16. Genes with significant and directionally shared differential gene expression after FOXA1 knockdown in H1819 and H1781 that are also near a FOXA1-bound region in 14q-amplified cells.

Table S17. DGIdb query results from candidate FOXA1 targets.